DOI: 10.7251/QOL2403117H **UDC:** 669.255:552.323.4/.5

Original scientific paper

Mineralogical and Geochemical Peculiarities of Rare Metal Granite Tillik (Laouni, Central Hoggar, North Africa)

Ahmed Hamis[1], Ali Makhlouf[1], Mokrane Kesraoui[2], Aissa Benselhoub[3], Elfahem Sakher[3,4], Stefano Bellucci[5]

[1]*Geological Sciences Department, FSBSA, Mouloud Mammeri University of Tizi-Ouzou, Tizi-Ouzou, Algeria; ahmed.hamis@ummto.dz; ali.makhlouf@ummto.dz*

[2]*Metallogeny and Magmatism Laboratory, (USTHB), Algiers, Algeria; mkesraoui@gmail.com*

[3]*Environmental Research Center (C.R.E); Annaba, Algeria; benselhoub@yahoo.fr*

[4]*Energy Environment and Information System (LEEIS), Department of Material Science, Faculty of Science and Technology, African University Ahmed Draia, Adrar, Algeria; elf.sakher@univ-adrar.edu.dz*

[5]*INFN-Laboratori Nazionali di Frascati Via E. Fermi 54, 00044 Frascati, Italy; bellucci@lnf.infn.it*

ABSTRACT: The Pan-African orogeny (800-570 Ma) is thought to have been the last event to affect this vast Hoggar region, while the post-collisional phase of the Pan-African chain (650-570 Ma) continued until (520 Ma) and saw the emplacement of numerous granitic plutons known as "Taourirt" for their potential sources of rare metals. In the central Hoggar, the latest magmatic episodes, represented by albite-topaz (AT) granites, are associated with Sn-Wn mineralization. These granites, which have undergone different degrees of evolution, are currently classified as Rare Metal Granite (RMG). In the Laouni terrane, the Tillik massif outcrops as a small flattened dome, backed by an NNE-SSW-trending accident. It is embedded in highly metamorphosed terrain and regional porphyroid biotite granite. The massif mainly comprises central green granite and leucocratic topaz albite granite, occupying the rest of the dome. Stockscheider pegmatites and greisens mineralized with cassiterite and wolframite occur around the edges of the massif, highlighting the area's significant mineralization potential alongside the granites. Furthermore, the granites are leucocratic and have a mineralogical composition consisting of albite and quartz with snowball structures, which is characteristic of RMG. They are phosphorus-poor, peraluminous, and show relatively flat rare-earth spectra with a strong negative Eu anomaly. The geotectonic sites show that the various samples are projected into the collisional intraplate granite domain, highlighting the transition from the post-orogenic to the anorogenic domain. This study aims to characterize the granites of the Tillik massif petrographically, mineralogically, and geochemically, compare them with the Hoggar rare-metal granites "Ebelekan and Rechla" and with the world-renowned reference granites "Beauvoir and Yichun," and determine whether or not they contain rare metals such as Li, Be, Nb, and Ta.

Keywords: Topaz granites, Columbo-tantalite, RMG, Tillik massif, Laouni, Hoggar, Algeria, Amazonite Granite, Post-Orogenic Granite

INTRODUCTION

The Tillik massif is located approximately 230 km southwest of Tamanrasset, at the southern border of the Tin Begane terrain. This massif of 1.5km x 1km is part of a set of post-orogenic granitic intrusions forming small-aligned domes along a regional NE-SW fault (Fig. 1).

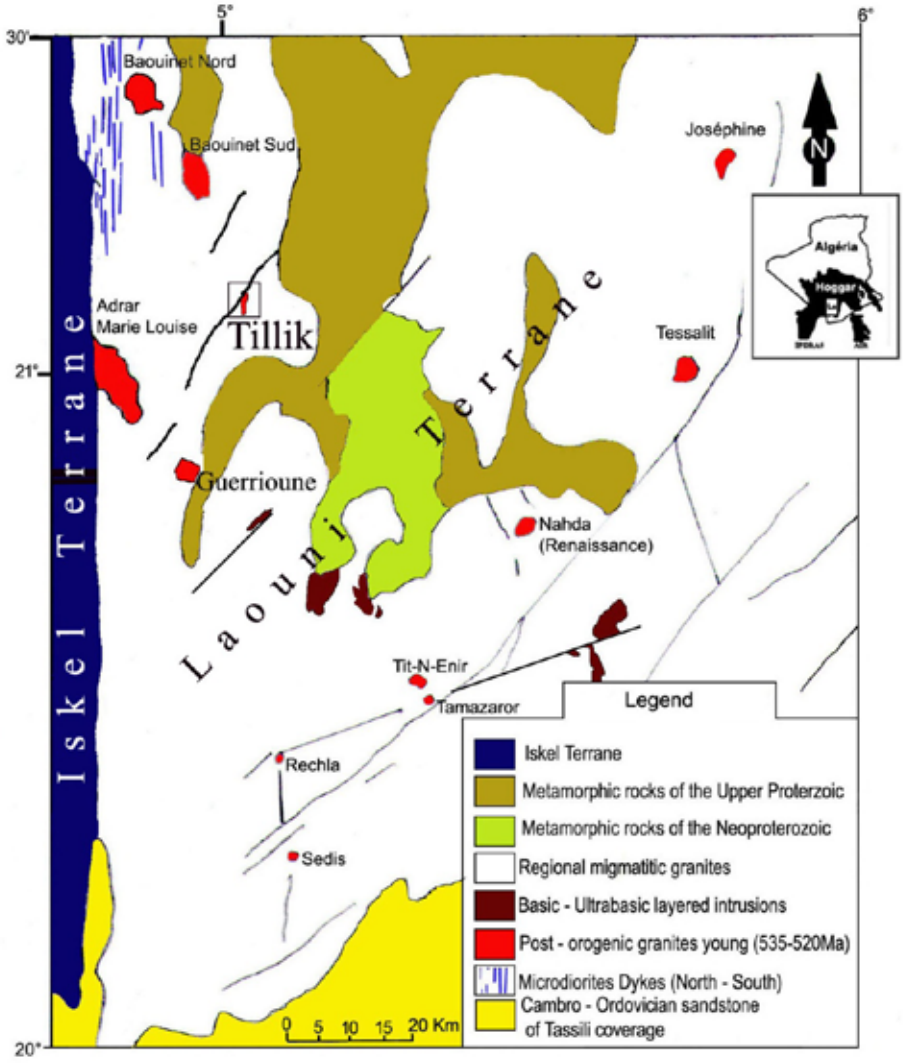

Fig.1. **Location** of the study area.

The Geological and Mining Research Office[1] (BRGM) discovered the Tillik massif in 1959-1960 during a geological mapping trip, in which several minerals have been identified such us Topaz, beryl, Fluorite, and wolframite. The National association of Research and Mining Exploitation SONAREM[2] (1969-1971, 1974) performed systematic geological prospecting and established consequently, a 1:20,000-scale geological map, emphasizing its potential for rare metals.

This study aims to emphasize the unique features of the Tillik granite formation, including its mineral composition and petrographic traits, and explore the geochemical characteristics of the primary, trace, and Rare Earth Elements (REE) present in this formation to determine its typology and compare it to other known examples of Rare Metal Granites (RMG). Moreover, this study aims to provide insight into the geotectonic context of the Tillik granite massif.

MATERIALS AND METHODS

To investigate the mineral phases that constitute the Tillik massif, samples were taken from uncovered polished thin sections, i.e., around twenty (20) thin sections representative of the different facies of the massif studied, prepared at the National Office for Geological and Mining Research (ORGM[3]) in

[1] Bureau de Recherche Géologique et Minière
[2] La Société Nationale de Recherches et d'Exploitation Minières
[3] Office National de la Recherches Géologiques et Minières

Boumerdès. Rock powders, including ten (10) sample powders produced at the Faculty of Earth Sciences, Geography and Territorial Planning Laboratory, University Of Science and Technology Houari Boumediene (USTHB) Algiers.

The following analytical techniques were used; the Transmitted Light Optical Microscope (TLOM) for the study of thin sections, Scanning Electron Microscope (SEM) to identify mineral inclusions that cannot be identified by polarized microscopy, and Electron Microprobe Analyses (EMPA). EMPA were performed using the SX 100 CAMECA (analytical conditions 15Kv, 12nA, and counting time 15s). SEM image by S-4800, signal name: YAGBSE, accelerating voltage: 20Kv, emission current: 9.8Na and counting time 20 to 40s. The observations were performed at the Geo-Ressources Laboratory, Department of Geology, Nancy University (France). Inductively Coupled Plasma Atomic Emission Spectroscopy (ICP-AES) and Inductively Coupled Plasma-Mass Spectroscopy (ICP-MS) methods were used for primary, trace, and rare earth element analyses conducted at Centre de Recherches Pétrographiques et Géochimiques (CRPG) in Nancy (France).

RESULTS AND DISCUSSION

Post-Orogenic Granites

The Hoggar is characterized by the "Taourirt" event closing the Pan-African orogeny stages. Different granitic plutons were emplaced with varying petrographic, geochemical, and age characteristics from 539-523Ma (Azzouni-Sekkal et al., 2003). They are distributed over three distinct provinces: **Silet** (Iskel terrane), **Tamanrasset**, and **Laouni** (Laouni terrane) (Azzouni-Sekkal, 1989; Azzouni-Sekkal et al., 2003; Boissonnas, 1973). In the Iskel terrane, four main groups have been defined (Azzouni-Sekkal & Boissonnas, 1993), namely:

- **group GI:** Biotite amphibole monzogranite is moderately fractionated, shows weak negative anomalies in Europium (Eu), and is lightly enriched in light Rare Earth Element (REE).
- **group GIIa:** Biotite amphibole monzogranite and syenogranite are less fractionated models with pronounced negative anomalies in Eu.
- **group GIIb:** The Taourirt suite has two highly evolved types - alkali feldspar granites and alaskites. The latter contain pure albite and lithium micas, similar to the Pan-African Tuareg (PAT) found in Tamanrasset.
- **group GIII:** The hypersolvus syenites and granites are little evolved

A hyperaluminous magmatic episode of crustal origin (PAT) in the Laouni terrane of the Tamanrasset region occurred between 539 and 525 Ma (Cheilletz et al., 1992). The latter was succeeded by late magmatism, represented by more evolved albite-topaz granites (**AT**), associated with SN-WN mineralizations (Chalal & Marignac, 1997; Cheilletz et al., 1992; Moulahoum, 1988).

These latest magmatic manifestations (**AT**) have changed to varying degrees and are currently classified as Rare Metal Granites (RMG). For instance, the Ebelekan massif (Low P, High T) is believed to be a representative example of this classification for the entire Hoggar region (Kesraoui, 2005; Kesraoui & Nedjari, 2002; Nedjari et al., 2001). These granites also show great similarities with the so-called evolved RMG known worldwide; France: (Cuney et al., 1992; Raimbault et al., 1995), Yichun; China : (Huang et al., 2002; Lin Yin et al., 1995), Pleasant Ridge ; Canada : (Taylor, 1992), and the SE desert of Egypt: (Kamar, 2015; Masoud & Shahin, 2015; Mohamed, 2012).

In the Laouni region, occurs numerous small post-orogenic granitic domes namely Guerrioune, Tit Enir, Nahda, Sédis, Tamazaror, Tessalit, Rechla (510±15 Ma, dating due to a pegmatite vein, (Gravelle,

1972) as well as the studied Tillik massif. These granitic domes are often associated with wolfram, tin, beryllium, niobium, tantalum, and rare metal mineralizations.

Rare Metal Granites (Rmg)

Rare Metal Granites (RMG) are highly sought-after for their potential to contain rare metals such as Ta, Nb, W, Sn, Li, Be, Rb, Cs, U, and Zr. They are generally characterized by the most fractionated, latest, and apical terms and are emplaced in the late Archean to an-orogenic environments from the Late Archean to the Tertiary. They can take various forms, such as isolated granitic stocks (Beauvoir, France), small granitic domes (Laouni, Algeria), microgranitic veins or quartz-keratophyres (Mongolian ongonites), rhyolites (Richemont, France), volcanic tuffs (Spor Mountain, USA). The latter contains the world's largest reserves of beryllium (bertrandite). Granites containing rare metals can be classified into three different categories:

a. **Peralkaline RMG with [Al/(Na+k) <1]**
   It has low P, high rare REE, and a low Ta/Nb ratio. These granites are weakly enriched in Li, hence the reduced presence of lithium micas.
   These granites correspond to two types: the sodic amphibole-albite granites of the agpaitic class of (Kovalenko, 1977) and the highly fractionated granites of type A1.
b. **Phosphorus-rich peraluminous RMG with [Al/(Na+k)> 1.15]:**
   Phosphorus is present in apatite, amblygonite, montebrasite minerals, and feldspars. Low REE, Th, Y, Hf, Sc, and Pb levels characterize these RMG. Its Ta/Nb ratio is ≥ 1.
   Leucogranitic plutons containing muscovite-biotite are associated with this type of RMG found in post-orogenic continental collision chains.
c. **Phosphorus-poor peraluminous RMG with [1<Al/(Na+k)< 1.15]:**
   Compared to the two previous groups, they have intermediate REE, Th, Y, Zr, Hf, and Th contents. Their REE spectra are typically flat, with prominent negative anomalies in Eu. This type of RMG is found in post-orogenic geotectonic environments.

Geological setting

The Laouni terrane (Fig.1), is an integral part of the LATEA [Laouni, Azroun' fad, Tefedest, Egéré - Aleksod and Aouilène,] metacraton (Liégeois, 2019), which is characterized by a stack of NW-SE trending nappes and abundant Pan-African anatexis granitoids associated with poly structured gneissic formations of the Paleoproterozoic basement, with more or less abundant amphibolite and granulite facies dated at 2000 Ma (Peucat et al., 2003).

In this area, a tectonic unconformity separates two distinct Paleoproterozoic metamorphic ensembles (Bertrand, 1974):

- A lower gneissic unit (**Arechchoum series**) dominated by orthogneisses, leptinites, and quartzo-feldspathic gneisses, associated with rare metasediments in the amphibolite to granulite facies.
- An upper gneissic unit (**Aleksod or Egeré series**) consisting mainly of paragneisses and amphibolite-facies metasediments (quartzites, marbles, and amphibolites).
- Relics of small Pan-African basins, unconformably with the upper gneissic unit, are formed by greenschist-facies referred to volcano-sedimentary formations.

These complexes are intruded by three granite groups: pre- to syn-tectonic anatexic granites of the "Anfeg" type (615 Ma), late-tectonic granites of the Tiferkit type (580 Ma), and the Laouni granites, including the Tillik massif, were emplaced at the end of the Pan-African orogeny. Mafic and ultra-mafic intrusions of mantle origin were emplaced during the post-collisional period (Cottin et al., 1998).

Petrography

The Tillik massif is mainly composed of central greenish amazonite granite, a small spike of leucogranite porphyritic microgranite in the NNE part, and leucogranite-topaz albite granite occupying the rest of the dome. Moreover, the boundaries between these granites are not well-defined.

Stockscheider-type pegmatites surround the massif's northeastern part, accompanying the granites. Mineralized greisens and a quartz vein network are found in the northwest and southeast parts of the massif (Fig. 1 and 2).

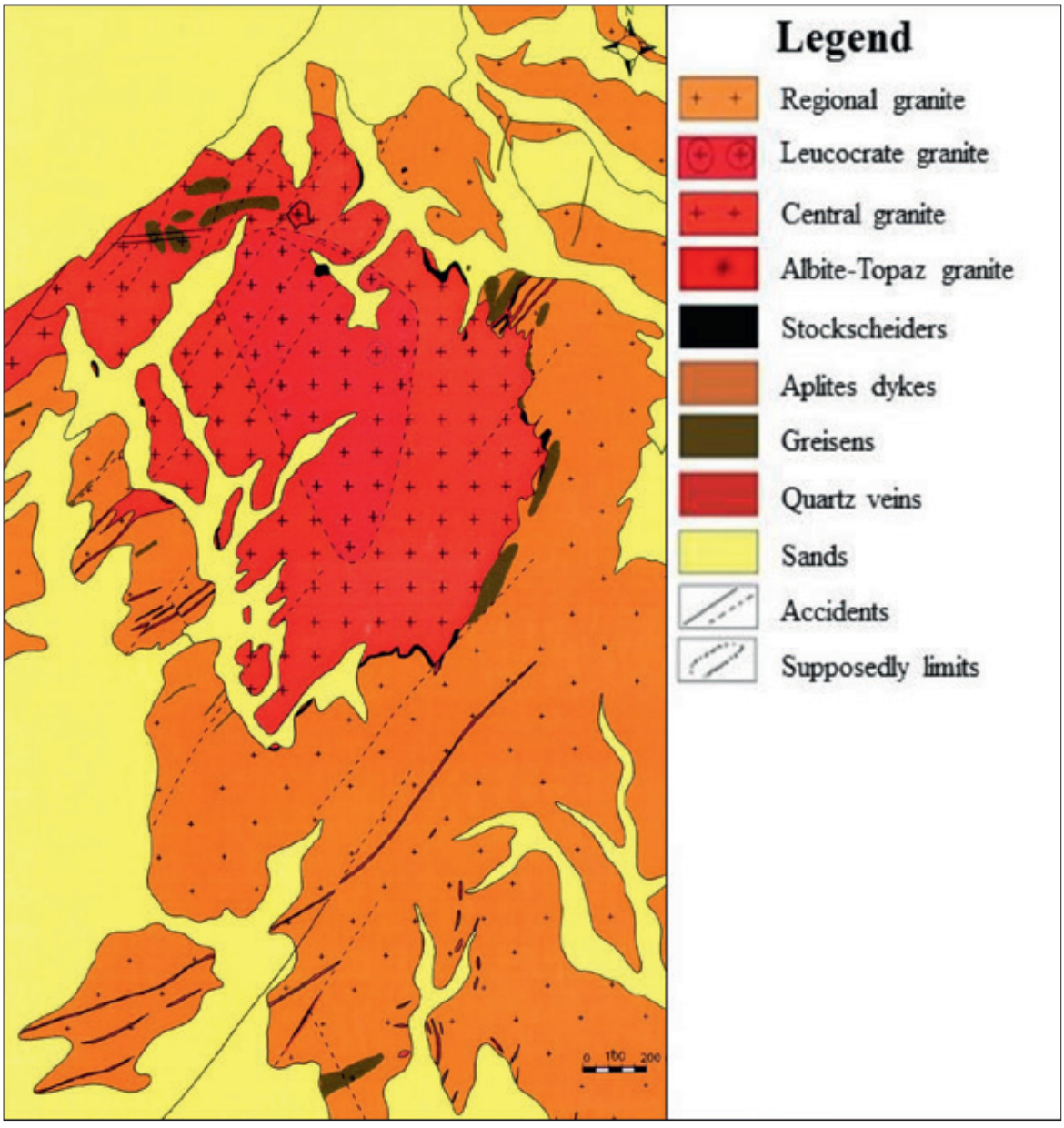

Fig. 2. Geological map of the Tillik area made from a drawing assembly (modified from (SONAREM, 1974)).

Central amazonite granite

It is characterized by a green color mainly due to the abundance of the microcline variety of amazonite. It is medium-grained, equigranular granite primarily consisting of a high-potassium feldspar matrix. In this matrix, well-developed globular quartz and black micas (zinnwaldite) are regularly scattered throughout the rock (Fig. 3b).

The microscopic analysis shows that the central granite has a grainy texture and consists mainly of quartz, with microcline more abundant than orthoclase, weakly pleochroic mica (zinnwaldite) with cassiterite inclusions, and albite. The latter has three generations:

- A first, early generation found in small laths in orthoclase, mica, and quartz. In the latter, albite displays a "snowball" texture characteristic of advanced rare-metal granites.
- A second generation of interstitials in automorphous laths with characteristic polysynthetic macles.
- A third generation in small-budding crystallites in microcline. This last generation of albite would be replaced by microcline and amazonite varieties.

The same phenomenon is observed in the amazonite leucogranites of Xinjiang in NW China (Gu et al., 2011).

The microcline, amazonite variety would replace this last generation of albite. This same phenomenon is observed in the amazonite leucogranites of Xinjiang in NW China (Gu et al., 2011). Topaz and Fluorite are rare.

Microscopically, the amazonite variety displays the same characteristics as microcline, except for the presence of Rb and Cs impurities in the crystal lattices. Microprobe analysis of a microcline yielded 0.02% Cs and 0.09% Rb.

The opaque minerals represent accessory minerals. They come in various forms, most often in the form of small, rounded, or scattered rods. Furthermore, some produce pleochroic halos. They are located in micas, following or crossing cleavage planes. They can also be found in quartz, feldspar, and topaz. These opaque minerals have been studied mineralogically by scanning electron microscope and microprobe (Hamis et al., 2021).

Albite - topaz granite

This highly leucocratic granite shares the same features as the preceding one. However, it appears to be whiter due to a decrease in microcline and an increase in albite and quartz. This granite also contains a relatively large amount of topaz (Fig.3c).

Under the microscope, the granite displays the same features as the central granite. However, we have observed certain peculiarities in the area. Firstly, the grain size appears to be finer than the surrounding area. Secondly, there is a significant decrease in potassic feldspar while the proportion of albite has increased. The topazes are also more extensive and abundant, as shown in (Fig. 3e). However, the proportions of micas remain the same. The characteristic "snowball" structure can be seen in (Fig. 3f).

Porphyritic microgranite

It outcrops as a small point in the northeastern part of the massif. Its spatial relationships with the surrounding topaz albite granite are unclear, but it appears to be intrusive. This light-colored granite (leucocrate) shows phenocrysts of globular quartz and feldspars. It is interspersed with albites and white micas.

Observations under the microscope show that the rock has a porphyritic micrograiny texture. Quartz appears in large, often fissured, automorphous to sub-automorphous patches up to 2mm. It shows magmatic corrosion structures and contains small plagioclase laths with small quartz crystals in inclusion, often forming a "snowball" structure.

Pegmatites

They often outcrop in zones with few centimeters in diameter inside granites. They feature large crystals of quartz, potassium feldspar, topaz, and disseminated micas. All these minerals are embedded in a feldspathic matrix.

Under the microscope, the rock has a pegmatitic texture represented mainly by automorphic to sub-automorphic phenocrysts of quartz and albite. Potassium feldspars (microcline, orthoclase), micas (zinnwaldite and muscovite), and topaz are scarce. Quartz contains embedded albite laths.

Phenocrystalline microcline is often perthitic. When in contact with micas, the latter interpenetrate along the cleavage planes of potassium feldspar. They also contain albite laths and fine quartz crystals. Oxides underline cracks. Orthoclase often occurs in smaller patches and contains albite laths and small xenomorphic quartz crystals.

Weakly pleochroic zinnwaldite, often in large patches, comprises inclusions of oxides, muscovite, and albite crystallites.

The stockscheiders

Stockscheider-type pegmatite comprises mega-crystals of potassic feldspars, mostly feathery with disseminated micas. The whole is immersed in a matrix of potassium feldspars and quartz (Fig. 3d).

Under the microscope, sub-automorphic phenocrysts of perthitic orthoses, which took their time to crystallize first, can be seen. They contain quartz, micas, and albite in fine laths. The medium-sized equigranular quartz occupies the cavities between the potassium feldspar phenocrysts. They often show signs of magmatic corrosion. Inclusions include Fluorite and iron oxides. Micas in small, abundant patches are moderately pleochroic and occupy the voids between quartz crystals. These micas contain needle-like rutile, which are often invaded by oxides, and are sometimes fully substituted.

Topaz is relatively abundant and fills the interstices. It occurs in sub-automorphic patches up to 02mm in size. It also contains fine mica crystals.

The greisens

They are found in the northwestern and south-eastern parts of the massif (Fig. 2). They occur as lenticular bodies and rarely as veins. The stone is dark gray. The mineralogical composition is quartz, black micas, and oxides (Fig. 3a).

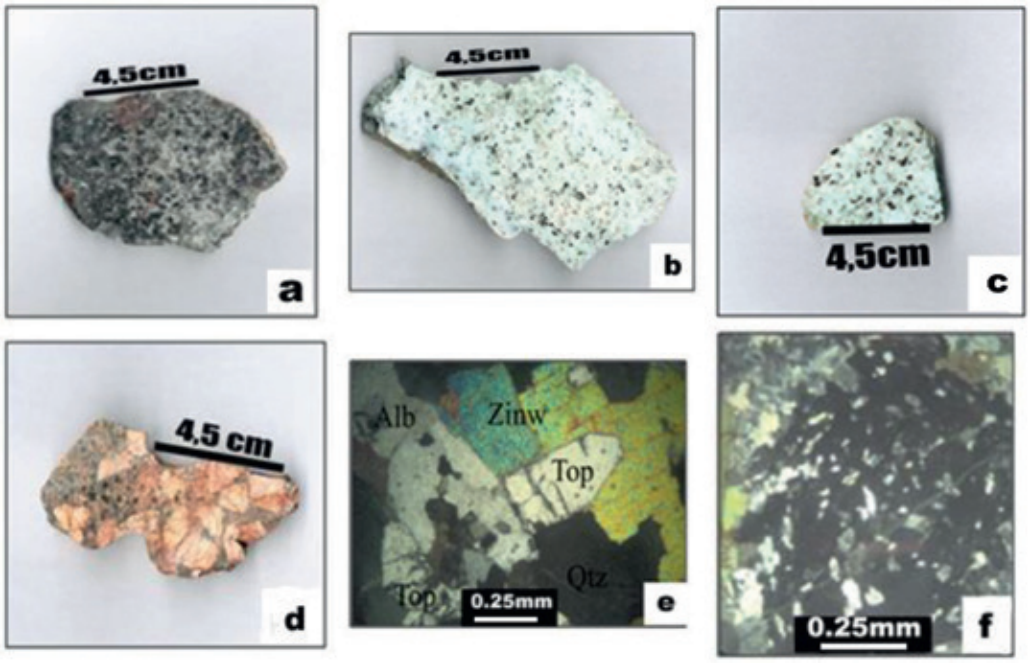

Fig. 3. Granite greenish central microcline, Greisens (a) amazonite variety (b), Granite albite topaz (c), Stockscheider "pegmatite feather" (d), Granite albite topaz microscopy (e), snowball structure of albite topaz granite (f).

Mineralogy

The micas in Tillik granites are weakly pleochroic, occurring in irregular patches and rarely in automorphic sections. Micas are also found in cracks and inclusions. They contain numerous inclusions (albite, quartz, Fluorite, zircon, columbo-tantalite, monazite and topaz).

Observations with a scanning electron microscope show a muscovite-cored zinnwaldite (Fig. 7d).

The micas in the topaz albite granite show relatively high Rb, Li, and F contents (Table 1) and project into the zinnwaldite field. Greisens extend into the siderophyllite field: $K2^{XII}(Fe^{2+}{}_4Al_2)^{VI}(Si_4Al_4)^{IV}O_{20}(OH)_4$, (Fig. 4 a and b).

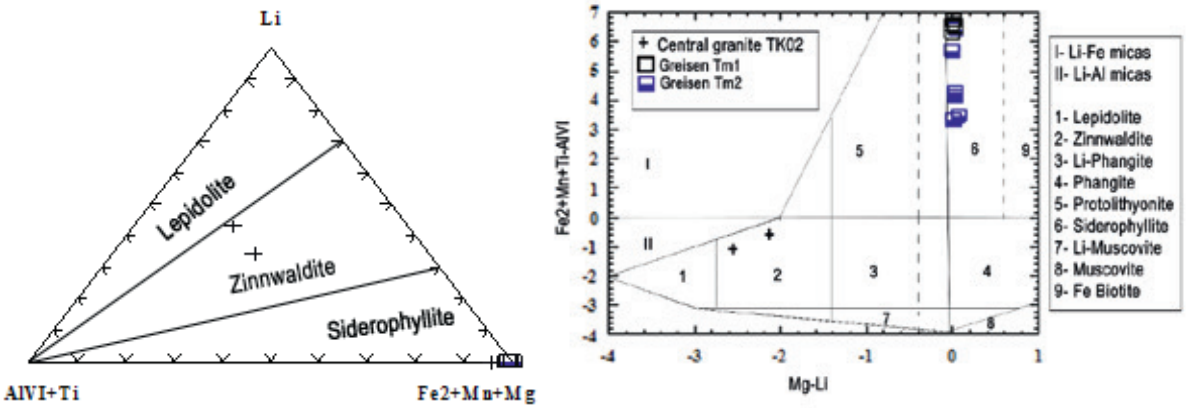

Fig.4. Distribution mica granite and greisen of the Tillik massif in the diagram (Tischendorf et al., 1997) a) Li-Al+Ti-Fe+Mg+Mn (Stone et al., 1988) ; and b) (Mg-Li) – (Fe+Mn+Ti-AlVI) (Tischendorf et al., 1997).

Topaz

Relatively abundant in these facies, it often occurs in large automorphic to sub-automorphic patches up to 5mm in size (Fig. 3e).

Topaz has substantial relief and is criss-crossed by numerous fractures underlined by oxides. When these fractures are open, they are filled with micas, quartz, and albite.

Inclusions include albite crystallites, fine columbo-tantalite rods, and fine quartz crystals. Topaz grades in topaz granite are higher in fluorine (F: 21.45) and lower in silica (SiO_2: 31.36), while the opposite is true in the case of greisens. They are lower in fluorine (F: 13.08) and higher in silica (SiO_2: 33.04) (Table 1).

Table 1. Topaz analysis of the Tillik massif (*TK02: Central granite; TM1 and TM2: Greisen*)

Sample	TK02-A	TM1	TM2	TM2	TM2
Analysis %	41	35	19	21	24
SiO_2	31.368	33.392	33.381	32.449	33.041
Al_2O_3	56.408	56.751	57.263	57.516	57.047
F	21.457	14.151	13.081	14.149	13.226
O=F	-9.01	-5.94	-5.49	-5.94	-5.55
Total	100.22	98.35	98.23	98.17	97.76
base O_2	5	5	5	5	5
Si	0.965	0.999	0.993	0.974	0.990
Al	2.046	2.001	2.009	2.035	2.014
F	2.088	1.339	1.231	1.343	1.253
OH	-0.088	0.661	0.769	0.657	0.747
F/F+OH	1.044	0.669	0.616	0.672	0.626
Total O_2	2.704	2.781	2.796	2.772	2.778
Structural Formula of topaz : $Al_2SiO_4(OH,F)_2$					

Accessories

Columbo-tantalites

Nb and Ta are accessory minerals disseminated in granites, greisens, and pegmatites. They occur mainly as inclusions in micas. Columbo-tantalites are characteristically rod-shaped and rarely prismatic. They vary in size from 20 µm to 120 µm, occasionally with fractures, and contain zircon inclusions.

Under the scanning electron microscope, they display a relatively well-expressed zonation of shade, with the core of the crystals darker than the edges, which is due to the heterogeneity of their chemical composition underlined by the substitution between the pairs of significant elements: Nb → Ta and Fe → Mn.

Such zones, whose contours are more or less regular, are represented by a dark core (enriched in Nb) evolving towards a light periphery (enriched in Ta) (Fig. 5).

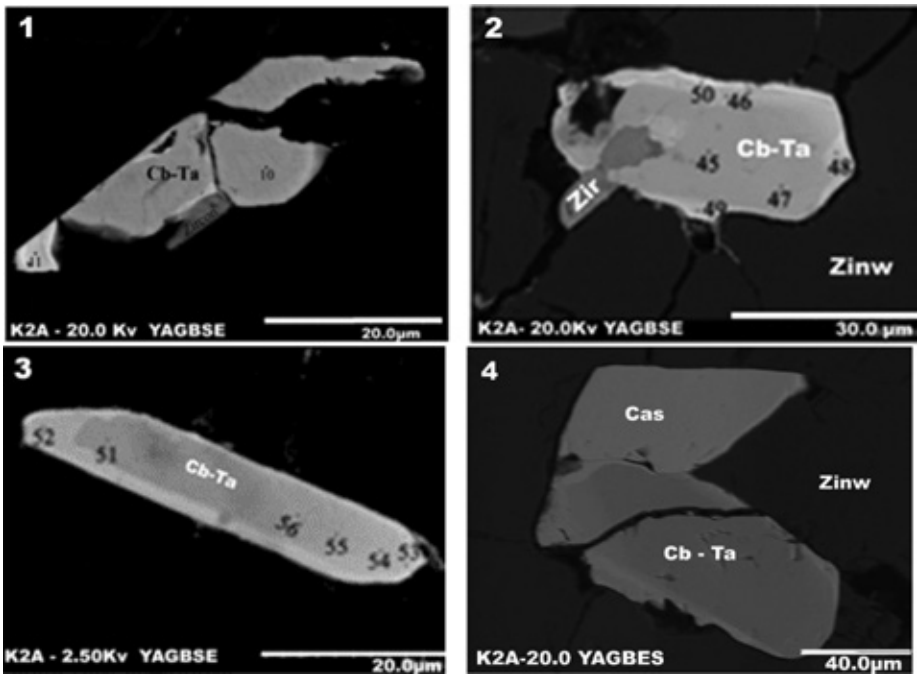

Fig. 5. Some forms of Columbite-tantalites of the Tillik massif analyzed by SEM. Abbreviation: *(Cb-Ta: Columbo-tantalite, Zir: Zircon, Zinw: Zinnwaldite, Cas: Cassiterite)*

On the chemical aspect

Central granite columbo-tantalites are richer in niobium than tantalum. They have high titanium contents and are slightly more manganiferous than ferriferous (Table 2). Columbo-tantalite is zoned with a ferro-columbite core enriched in Mn and a manganocolumbite edge, demonstrating an evolutionary trend towards manganotantalite. The transition from the core to the rim is marked by an apparent hiatus in the increase in Mn/Mn+Fe and Ta/Ta+Nb ratios (Fig. 6).

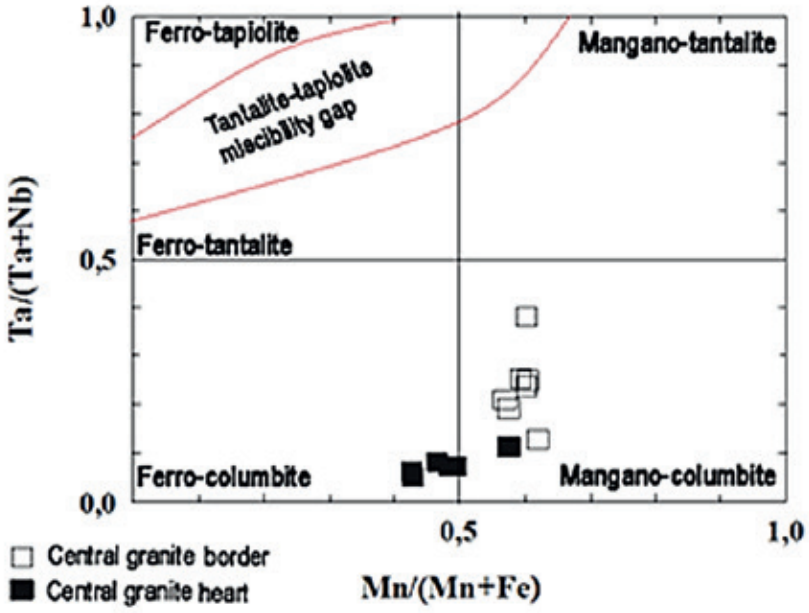

Fig. 6. Columbite-tantalite compositions of the central ferro-columbite granite, at the limit of manganese-columbite.

Table 2. Analysis of columbite-tantalites From the Tillik massif

DataSet/ Point	TK02-A1/10	TK02-A2/45	TK02-A2/47	TK02-A3/51	TK02-A3/54	TK02-A3/55	TK02-A3/56	TK02-A1/11	TK02-A2/46	TK02-A2/48	TK02-A2/49	TK02-A2/50	TK02-A3/52	TK02-A3/53
	Heart (gray area)							**Border (light area)**						
TiO_2	1.22	1.19	1.01	1.09	0.89	0.95	1.02	1.55	1.46	1.28	1.77	2.04	1.33	1.22
MnO	8.73	8.74	9.38	10.03	11.96	11.32	9.02	11.50	10.69	11.36	11.62	10.55	10.82	11.47
FeO	11.69	11.93	11.01	10.54	7.55	8.54	9.66	8.01	7.92	7.54	7.57	6.99	8.16	7.24
Sc_2O_3	0.24	0.27	0.19	0.27	0.22	0.22	0.23	0.40	0.34	0.40	0.48	0.59	0.37	0.34
Nb_2O_5	**68.52**	**67.33**	**66.75**	**66.37**	**62.07**	**63.70**	**64.27**	**49.73**	**55.19**	**51.69**	**49.06**	**37.67**	**53.93**	**55.63**
SnO	0.19	0.16	0.27	0.05	0	0.12	0.16	0.29	0.06	0	0.21	0.08	0.06	0.14
Ta_2O_5	**6.34**	**7.50**	**9.11**	**8.85**	**15.09**	**13.25**	**8.35**	**27.86**	**21.42**	**26.97**	**26.56**	**38.50**	**23.58**	**20.82**
WO_3	1.25	1.07	0.75	1.30	0.08	0.38	1.11	0.05	0.45	0	0	0	0.21	0
UO_2	0.13	0	0.23	0	0	0	0	0	0.12	0	0	0.08	0.132	0
Total	98.34	98.21	98.74	98.54	97.9	98	93.85	99.43	97.71	99.26	97.29	96.52	98.61	96.88
Moy. Nb				65.57							50.41			
Moy. Ta				9.78							26.53			

Monazite

Monazite is found in albite-topaz granite. It is automorphic, with well-defined outlines 150µm in size. It occurs as an inclusion in quartz and zinnwaldite, forming a pleochroic aureole, and in cracks in Fluorite.

Under the scanning electron microscope, monazite shows a remarkable dominance of cerium (Fig. 7c).

Cerianite

Cerianite is a cerium oxide of the general formula (Ce, Th) O_2, with other REE. The chemical composition of cerianite shows that CeO_2 can exceed 80% and ThO_2 5-6%. It also contains other REEs and traces of Nb and Ta.

The SEM-observed cerianite occurs in albite-topaz granite, as an inclusion in micas. It adjoins a columbo-tantalite rod (Fig. 7b) characterized by automorphic shape with corroded contours. Its size can reach 130µm.

An elemental map of the cerianite crystal was produced using Scanning Electron Microscopy (SEM). The crystal displays an even distribution of Ce, Pr, and Nd throughout. However, Th is mainly concentrated at the periphery, while La is primarily present at the core of the mineral. A buffer zone exists between cerianite and columbo-tantalite, enriched in P and likely monazite. The columbo-tantalite does not contain any of the analyzed elements, i.e., rare earths and P.

Fluocerite and melanocerite

These minerals were determined by SEM, and appear as inclusions in Fluorite. Fluocerite and melanocerite contain high levels of the radioactive elements of cesium and thorium. Melanocerite is a mineral with a low fluorine content (1.41) and very little La_2O_3 (0.00), but it is rich in P_2O_5 (5.22) and Ce_2O_3. On the other hand, fluocerite has a high concentration of fluorine (42.98) and low levels of alumina, phosphorus, and potassium.

Other minerals

Zircons are very abundant in the various facies of the Tillik massif. They are found in thin sections of quartz and, more often, in micas, where they develop pleochroic aureoles. Observations with SEM show that are present in several minerals such as micas, quartz, albite, topaz, Fluorite, and columbo-tantalite. The zircons have not been analyzed.

Apatite is a rare mineral observed under a polarizing microscope as fine automorphic rods in micas. Under the SEM view, apatite fills cracks in mica and zircon or as isolated crystals (Fig. 7c).

Conversely, Fluorite is often sub-automorphic and small, typically ranging from 30µm to 40µm. SEM analysis reveals that Fluorite includes very small albite laths and numerous zircons (Fig. 7a).

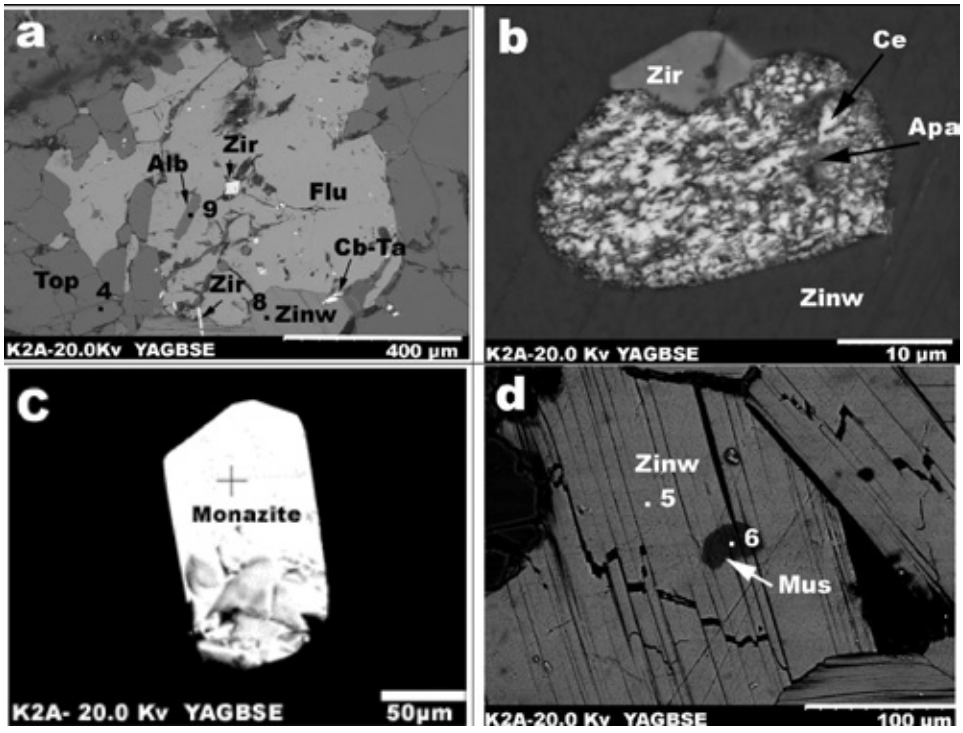

Fig. 7. Fluorite (Flu), Zinnwaldite (Zinw) and topaz (Top) association (a), Cerianite (Ce) and apatite (Ap) in zinnwaldite(b), Monazite (c) and Zinnwaldite with muscovite (Mu) core (d) using the SEM

Geochemistry

The petrographic and mineralogical analysis is reinforced by geochemical data to determine the location of the studied granites compared to the known rare-metal granites in the region, including major elements, REE, and trace elements.

Major elements

The Tillik massif granites are highly siliceous (73.41< SiO_2 <75.29), alkaline-rich (9.04< Na_2O + K_2O <12.59) and peraluminous (14.58 < Al_2O_3 <15.59).

MnO contents can generally be considered relatively high (0.03< MnO <0.10), and these differences are probably due to the abundance of micas and oxides in the various facies. The rocks of the Tillik massif are depleted in iron (0.41 < Fe_2O_3 < 0.54), calcium (0.28 < CaO < 0.06), phosphorus (0.04>P_2O_5>L.D), and titanium (L.D <TiO_2<0.01) (Table 3).

Fluorine was not detected, but lithiniferous micas (zinnwaldite) and topazes had high fluorine contents (2.78 < F < 7.55 and 13.08 < F < 21.45, respectively).

The Harker diagrams reveal a negative correlation between alumina, ferromagnesium, and silica, as opposed to alkalis and calcium, which increase with decreasing silica.

The A/CNK molar ratios of Tillik massif granites are greater than unity (1.5). These values characterize peraluminous granites in Shand's classification (Shand, 1927). This data is also supported by normative corundum values between 1.63 and 2.38. The ANK/ACNK diagram by (maniar & piccoli, 1989) confirms these findings, indicating that the granites analyzed fall within the peraluminous range.

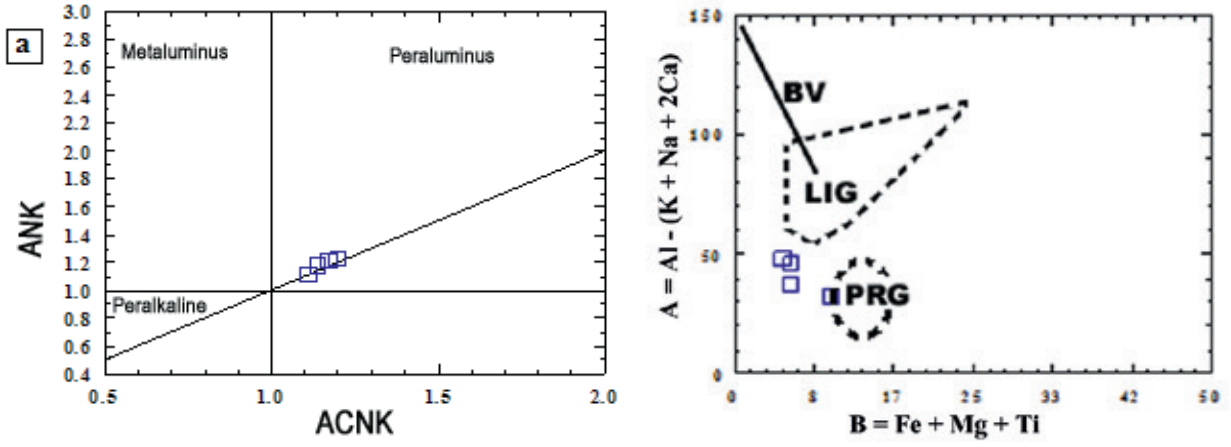

Fig. 8. Al_2O_3/ (Na_2O+K_2O) Tillik vs alumina to lime and alkalis Al_2O_3/Na_2O+K_2O+CaO after (Maniar & Poccoli, 1989), comparison with reference granites; [Bv: Beauvoir and LIG: Erzzebirge (Raimbault et al., 1995), PRG: Pleasant Ridge (Taylor, 1992)] in the A-B of (Debon & Lefort, 1988).

Table 3. Tillik granites majors' elements analysis

Samp.		TK 02	TK 03	TK 12	TK 04		TK02	TK03	TK12	TK04
SiO_2	%	73.41	75.29	73.96	68.17	**A/CNK**	**1.17**	**1.20**	**1.14**	**1.11**
Al_2O_3	%	15.59	14.58	15.45	17.22	**A/NK**	**1.21**	**1.22**	**1.17**	**1.11**
Fe_2O_3	%	0.54	0.41	0.49	0.65	K_2O/Na_2O	0.89	1.34	0.87	2.79
MnO	%	0.08	0.10	0.03	0.04	CaO/Na_2O+K_2O	0.03	0.01	0.02	0.00
MgO	%	< L.D	< L.D	< L.D	0.12					
CaO	%	0.28	0.13	0.23	0.06					
Na_2O	%	4.94	3.86	5.09	3.32					
K_2O	%	4.38	5.18	4.43	9.25					
TiO_2	%	0.01	0.01	< L.D	0.01					
P_2O_5	%	< L.D	0.04	0.02	< L.D					
PF	%	0.85	0.67	0.47	0.71					
Total	%	100.07	100.27	100.16	99.54					

Tk02: Central granite
Tk03: albite-topaz granite with pegmatite pocket
Tk12: Albite-topaz granite
Tk04: Pegmatite in albite-topaz granite

Trace elements

Tillik massif granites are poor in trace elements with large ionic radii (LILE): Ba, Sr, Y, and Zr. However, they are characterized by very high levels of Rb and Ga. Generally, Micas and feldspars control these elements. It is admitted that the "LILE" components behave normally for advanced granites. The levels of rare alkaline elements such as Be and Cs are relatively low and are primarily influenced by micas. However, lithium has not been analyzed (Table 4).

Table 4. Tillik granites trace elements analysis

Samples	Ba	Rb	Sr	Zr	Hf	U	Th	Cs	Ga	Y	Cr
TK 02	10.24	1355	15.64	23.84	3.492	1.436	13.58	9.609	47.39	11.96	113.3
TK 12	18.78	1122	8.815	19.91	3.289	2.701	13.14	4.047	53	3.391	184.1
TK 03	27.77	1509	5.497	21.96	3.937	1.929	7.552	1.498	47.52	4.257	74.14
TK 04	22.56	2290	10.21	4.585	0.847	10.94	4.467	11.32	60.11	0.763	185.3
Samples	**Be**	**Nb**	**Ta**	**W**	**Sn**	**Pb**	**Zn**	**Cu**	**V**	**Bi**	
TK 02	4.589	54.58	17.59	4.762	98.51	50.77	69.47	< L.D	3.229	0.932	
TK 12	3.741	46.93	31.39	9.682	115.7	38.69	28.04	< L.D	5.027	0.262	
TK 03	< L.D	60.83	25.64	5.851	53.27	37.39	122.5	< L.D	2.047	0.164	
TK 04	3.747	15.8	12.51	12.98	86.19	64.51	72.66	10.49	5.682	12.11	
Samples	Ni	Ge	Co	Mo	Nb/Ta	Rb/Sr	K/Ba	K/Rb	Zr/Hf	Th/U	
TK 02	11.2	4.882	0.648	3.431	3.10	86.63	09.08	00.06	06.82	09.45	
TK 12	11.81	4.235	0.711	5.495	01.49	127.28	05.00	00.08	06.05	04.86	
TK 03	8.646	5.444	< L.D	3.115	02.37	274.51	03.96	00.07	05.57	03.91	
TK 04	5.534	5.466	0.622	9.479	01.26	224.28	08.70	00.08	05.41	00.40	

The Ba/Rb ratio, ranging from 0.007 to 0.01, is relatively low and often related to Sn enrichment, a characteristic of highly differentiated, mineralized granites.

The triangular diagram (Rb/Sr/Ba) shows a high concentration of grades in the rubidium pole. It confirms their character as highly differentiated granites comparable to those of Ebélekan, Egele, and Nuweibi (Fig. 8).

Elements with high ionic charges (HFSE)

The element Sn has very high values. Although W occurs as wolframite with cassiterite in the gre-

isens at the top of the dome, it has very low values. Niobium grades are significantly higher than tantalum, and thorium grades are higher than uranium. In addition, the ratios (Nb/Ta) and (Th/U) are well above unity.

The levels of transition elements such as Pb and Zn are very high in the area. High levels of Cr and Ni suggest contamination due to assimilation from the primary and ultrabasic rocks in the region. By normalizing multi-element curves to the averages of the lower continental crust (McLennan, 2001), it is clear that the granites of the Tillik massif have positive anomalies for Rb, Sn, Ta, Nb, La, Y, and Zn. On the other hand, Negative anomalies are most notable for Th, U, Zr, Eu, Ba, and Sr (Fig. 9).

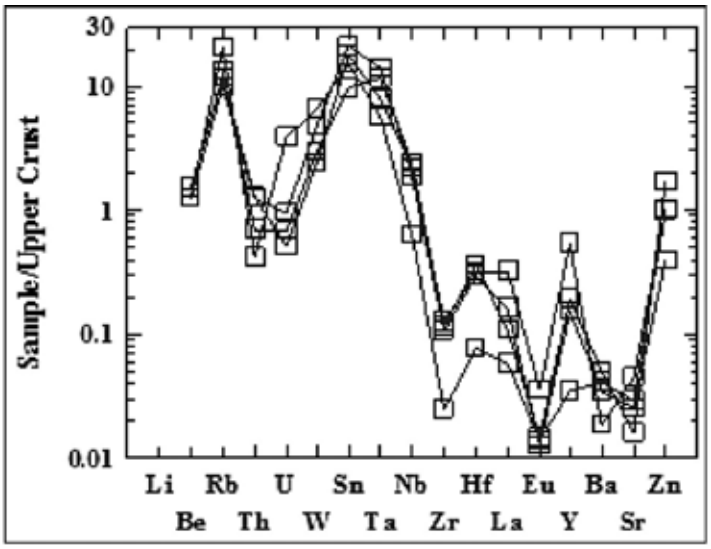

Fig. 9. Curves trace element contents normalized to the upper continental crust for the massive granite Tillik. The composition of the continental crust top is from (McLennan, 2001).

Rare Earths Elements

Accessory minerals like thorite, xenotime, uraninite, monazite, cerianite, and zircon often separate REE. These minerals are commonly found in Tillik granites. The central granite is highly enriched in REE, whereas the albite-topaz granites become increasingly depleted towards the periphery. The periphery region contains many pegmatitic zones with a REE sum ranging from 11.05 to 88.45. Data on REE indicate a decrease in concentration from the center to the edge of the massif (Table 5).

Table 5. Tillik granites rare elements analysis

Samples	La	Ce	Pr	Nd	Sm	Eu	Gd	Tb	Dy	Ho
TK 02	9.562	34.93	4.04	11.82	4.119	0.031	2.519	0.72	5.192	0.989
TK 12	4.836	16.17	1.957	5.152	1.672	0.011	0.852	0.247	1.762	0.321
TK 03	3.266	9.056	0.779	2.079	0.649	0.013	0.501	0.181	1.682	0.375
TK 04	1.743	5.564	0.447	1.097	0.277	0.012	0.196	0.051	0.397	0.083
Samples	**Er**	**Tm**	**Yb**	**Lu**	**Total**	**Eu/Eu***	**La/Yb_N**	**La/Sm_N**	**Gd/Yb_N**	**$TE_{1,3}$**
TK 02	3.599	0.902	8.745	1.289	88.45	0.03	0.76	1.46	0.24	1.57
TK 12	1.24	0.344	3.501	0.521	38.58	0.03	0.96	1.82	0.20	1.58
TK 03	1.498	0.371	3.644	0.536	24.44	0.07	0.62	3.16	0.11	1.43
TK 04	0.305	0.072	0.704	0.109	11.05	0.16	1.72	3.96	0.23	1.60

Rare-earth spectra (Fig. 10) demonstrate enrichment in the central granite (1), which is 60 times greater than chondrite standards. Moreover, the topaz albite granite (2) shows ten times the norm but is more depleted than the central granite. In contrast, the pegmatites (3) show a rare-earth spectrum below

10, with depletion progressing from the core to the periphery. This phenomenon can be explained by the leaching of rare earths by hydrothermal solutions towards the eroded summit parts of the massif. Rare earth spectra are relatively flat, with a pronounced Eu anomaly (0.03<Eu/Eu*<0.16).

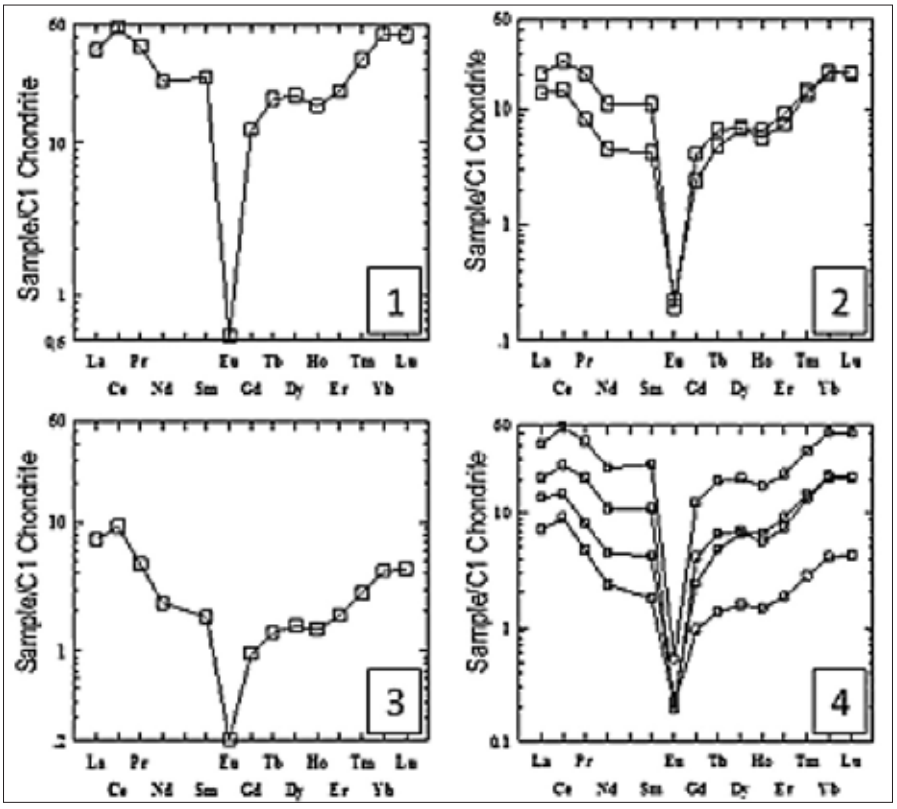

Fig. 10. Spectra of Rare Earth: central granite (1) topaz-albite granite (2) pegmatite (3) granites Tillik (4).

Geotectonic Site

The Tillik massif granites are projected into the domain of strongly fractionated alkaline granites (Fig. 13). According to (Pearce et al., 1984), geotectonic diagrams can be used to identify the location of various samples. In this case, the samples fall within the category of collisional intraplate granites (Fig.12 a,b). Additionally, the transition from the post-orogenic to the anorogenic domain can be highlighted using the R1-R2 diagram (Fig. 11).

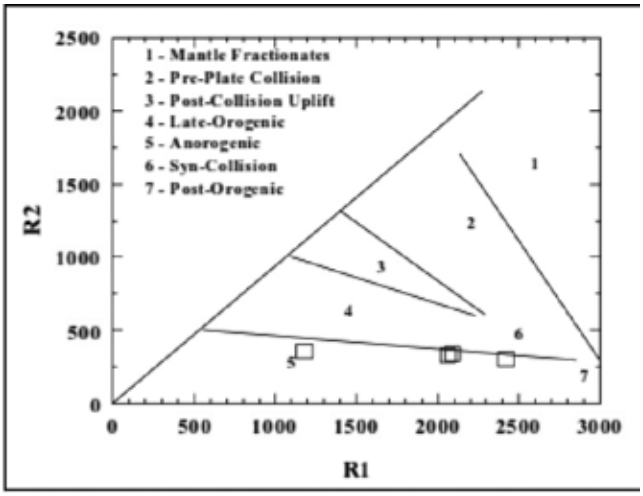

Fig. 11. Tillik granites mapped on the R1-R2 diagram (De la Roche et al., 1980). Fields shown are from (Batchelor & Bowden, 1985).

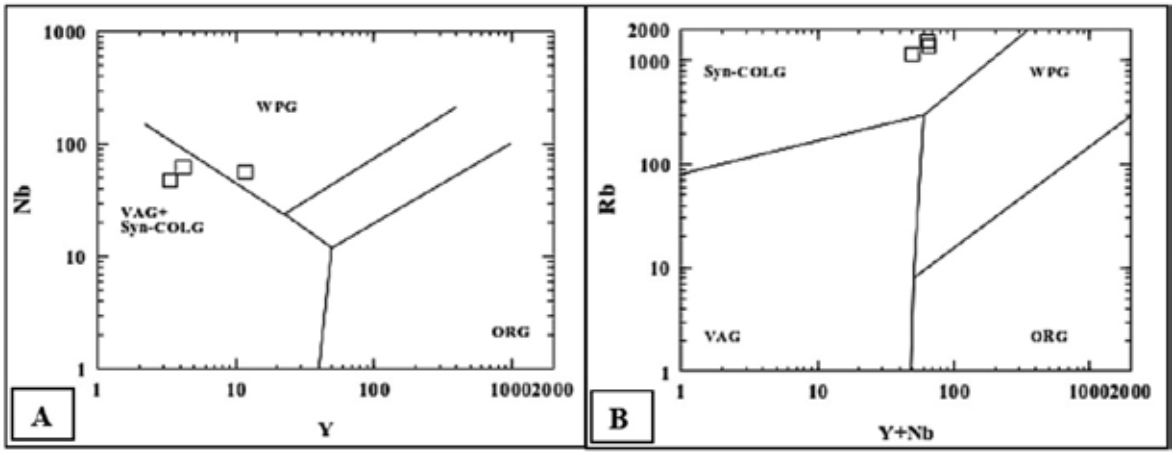

Fig. 12. Geotectonic mapping of the granites investigated in the (Rb vs Y+Nb in (a) and (Rb vs Y) diagrams by (Pearce, 1996) in (b). (COLG: Collision Granite; ORG: Ocean Ridgee Granite; VAG: Volcanic Arc Granite; WPG: Within Plate Granite)

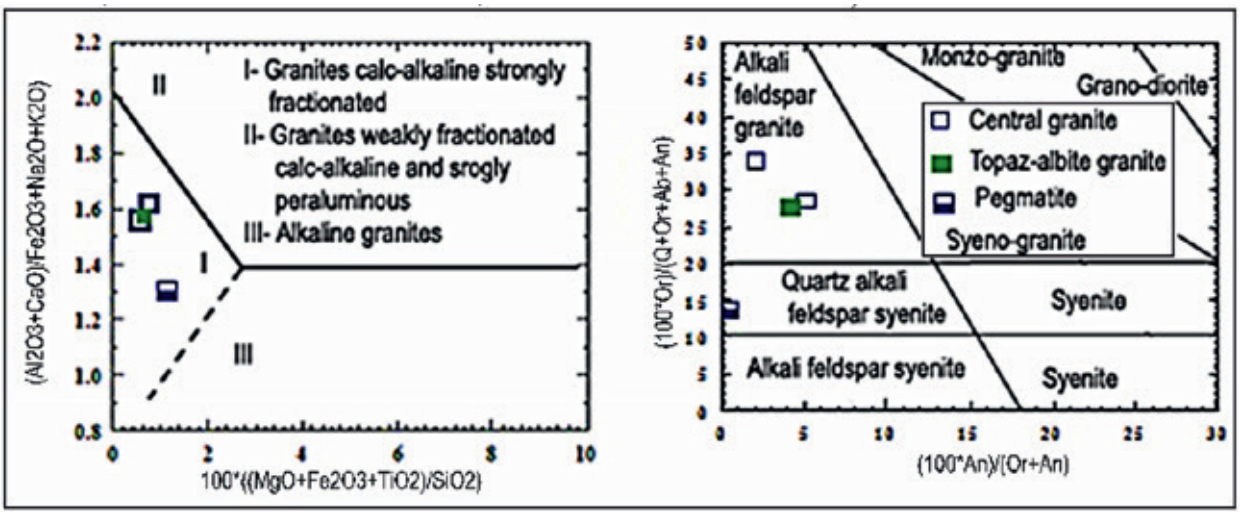

Fig. 13. Tillik granites are projected in the field of calc-alkaline granites strongly fractionated according to diagram of Sylvester (Sylvester, 1989).

Standard data (Diagram: Quartz- Albite- Orthose)

In the Q-Ab-Or diagram (Fig. 14), the representative points of the Tillik massif granites project between the 1- and 2% fluorine minimums at moderate water vapor pressure (3-5 kb). This suggests that they were formed at moderate levels in the crust. Furthermore, the pegmatite sample tends to approach the orthoclase pole.

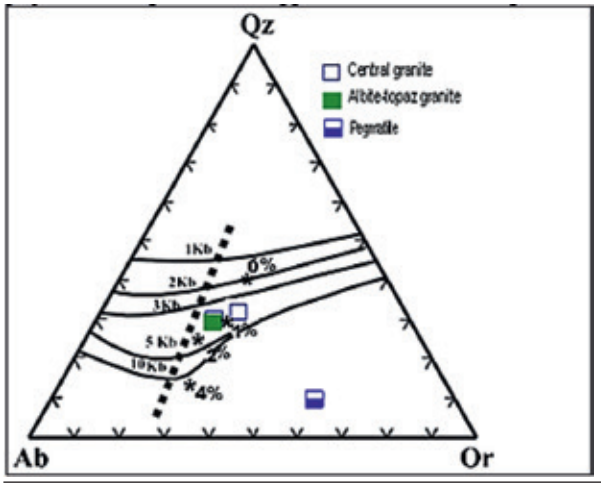

Fig. 14. Qz-Ab-Or ternary diagram; the dashed line represents the minimum melting points in the granite system at different water-vapor pressure; 1, 2, and 3 kb, after (Luth et al., 1964; Tuttle & Bowen, 1958); 5 and 10 kb, after (Luth et al., 1964); and 0,1,2,4% of fluor (Manning & Holthuis, 1981)

Comparison of Tillik granites with reference granites

Tillik granites show a regular evolution in the A-B diagram of (Debon & Lefort, 1988) (Fig. 15). They are more peraluminous and less ferromagnesian, although positioned in the same field as the Ebelekane and Tamanrasset granites, which show the opposite trend (Kesraoui & Nedjari, 2002).

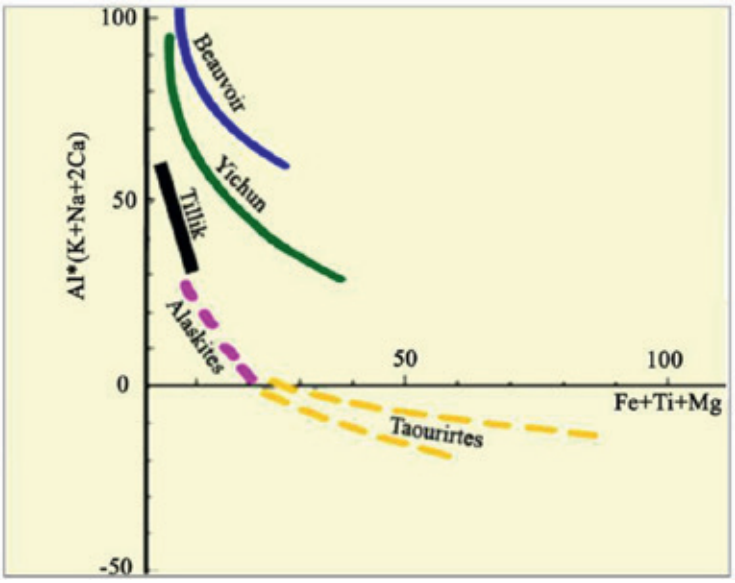

Fig. 15. Position of the Tillik granites in the A-B diagram by (Debon & Lefort, 1988). Alaskites and Taourirts (Azzouni-Sekkal, 1989), for comparison: (Beauvoir ; France: (Cuney et al., 1992; Raimbault et al., 1995), Yichun ; China :(Lin Yin et al., 1995)).

Overall, the granites of the central Hoggar occupy an intermediate position between the alaskites, "the most evolved granites of the Iskel terrane, Taourirt," and the most evolved and peraluminous Beauvoir granite. This fan-shaped arrangement suggests a mixture of two magmatic strains (Bouabsa et al., 2005). One of these would be peraluminous of the "primitive" Beauvoir type, while the other would match the more fractionated terms of the Iskel terrane. The absence of "Beauvoir-type" rare-metal granite in this terrane is due to the lack of peraluminous protoliths that could produce rare-metal granite magmas by partial melting.

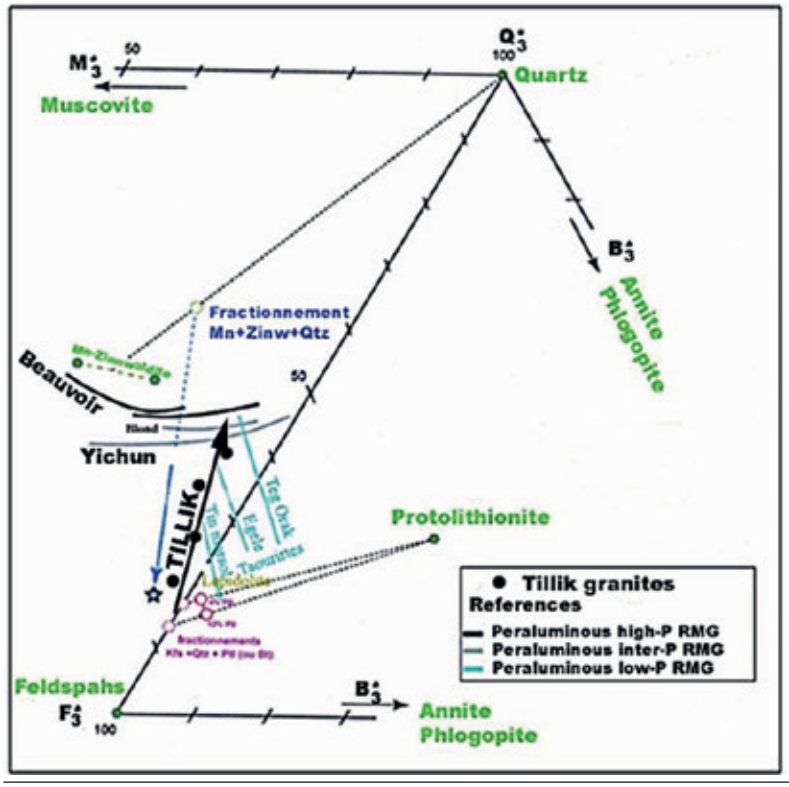

In the Q*3B*3F*3 diagram of (De la Roche et al., 1980) (Fig.16), the Tillik massif granites behave similarly as the albite-topaz-zinnwaldite (AZT) granite of Ebelekane. They display an inverse curve unlike the reference rare-metal granites (Beauvoir and Yichun).

Fig. 16. Q*3B*3F*3 diagram (De la Roche et al., 1980) for Tillik massif granitic facies, compared with reference granites (Beauvoir, Yichun, and Taourirtes du Hoggar).

DISCUSSION

The Tillik massif granites show homogeneous facies. From the center to the periphery of the massif, there is a noticeable decrease in potassium feldspar in favor of albite and a significant development of topaz, Fluorite, and lithiniferous micas. These facies are leucocratic granites, with a mineralogical composition represented by quartz with "snowball" structures characteristic of rare-metal granites.

From a mineralogical perspective, the columbo-tantalite deposits in this massif are enriched in niobium compared to tantalum (Nb>Ta). They exhibit a remarkable chemical zonation that records the history of magmatic crystallization. The cores of the crystals memorize the early magmatic stage (pre-stage), while the late magmatic stages are recorded by the margins.

From a geochemical perspective, the granites of the Tillik massif are strongly fractionated, peraluminous, poor in phosphate, and display relatively flat REE spectra with a pronounced anomaly in Eu. Moreover, geotectonic sites show that the different samples are projected into the intraplate granite of the collision domain and highlight the transition from the post-orogenic domain to the androgenic domain. Furthermore, these granites have crystallized rapidly at high temperatures and placed in shallow depths, constituting the most evolved suite of Alaskaites of the Taourirts of the Hoggar in the (Debon & Lefort, 1988) A-B diagram. Unlike the granites of reference (Beauvoir and Yichun), they exhibit an inverse curve in the Q*3B*3F*3 diagram of (De la Roche et al., 1980), suggesting a magma combination and blend.

One of the consequences of these mixing processes is that the Rare-Metal Granites in the Hoggar province (RMGh) are often poorly enriched in rare metals, as might be expected from their geochemical and mineralogical characteristics. Moreover, mixing can influence the specialization of some of these granites in other metals. For instance, the Be content of the Guerrioune, Tit n'Enir, Nahda, and Rechla beryl granites and pegmatites, and to a lesser extent, the Ebelekane, is related to the proportion of peralkaline magmas. This may also be the latest expression of "Taourirt" magmatism (Azzouni-Sekkal et al., 2003).

Based on the unusual geochemical behaviors, the RMGh, are believed to originate from a mix of different magmatic strains. These include a peraluminous strain that can produce RMG, corresponding to the most fractionated term of the "Taourirt" granites, and with a peralkaline tendency. Additionally, purely peralkaline granites of the same age can be found in the central Hoggar at Adjemamaye.

In the Hoggar rare-metal granite province, there are still no discoveries of the purest RMGh terms with significant mineralization so far. However, Rechla (with Li≈1600 ppm, Ta≈211ppm, Sn≈740 ppm, Zn≈200 ppm) and especially Ebelekane (with Li≈395 ppm, Ta≈306 ppm, Sn≈335 ppm) seem to be the least hybrid of the RMGh, according to (Kesraoui, 2005).

CONCLUSION

In this study, we presented the "Tillik" massif, one of the granite massifs of the Laouni region. The objective was to identify its petrographic, mineralogical, and geochemical characteristics.

At the end of this study, we can emphasize that the granites of the "Tillik" massif are to be classified among the Rare Metal Granites of Hoggar (RMGh) and come from a mixture of peraluminous, peralkaline magma which is the most fractionated of Taourirtes. However, they do not show any evidence of mixing magmas like those of Ebelekane and Rechla which are Tantalus granites. Unlike references, these granites are little enriched in rare metals (Beauvoir and Yichun).

In Hoggar, research on rare metals must be oriented towards post-orogenic granites with the potential to contain proven but little-studied mineralization, such as the Ebelekan massif located in the terrane (Assodé – Issalane) of orientalHoggar rich in Ta, the Guerioune massif for the Be-Ta-Nb, the and Rechla

for the Be-Li-Ta. The latter will be the subject of a subsequent study where its petrographic, mineralogical, and geochemical characteristics will be studied.

Acknowledgements
The authors would like to thank Professor C. Marignac from GeoRessources Laboratory, University of Nancy; and Dr Y. Fuchs of the Laboratoire Géomatériaux et Environnement (LGE), Paris Est Marne la Valée University (France).

Conflict of Interest
The authors declare no conflict of interest.

REFERENCES

Azzouni-Sekkal, A. (1989). Petrology and geochimy of granites type «Taourirt " : An example of magmatic province of the transition between the originical regimes and anorogenics, in Pan-African (Hoggar, Algeria). Universtiy of sciences and Technology Houari Boumedien, Algiers.

Azzouni-Sekkal, A., & Boissonnas, J. (1993). Une province magmatique de transition du calco-alcalin a l'alcalin; Les granitoides pan-africains a structure annulaire de la chaine pharusienne du Hoggar (Algerie). Bulletin de la Société Géologique de France, 164(4), 597-608.

Azzouni-Sekkal, A., Liégeois, J.-P., Bechiri-Benmerzoug, F., Belaidi-Zinet, S., & Bonin, B. (2003). The "Taourirt" magmatic province, a marker of the closing stage of the Pan-African orogeny in the Tuareg Shield : Review of available data and Sr–Nd isotope evidence. Journal of African Earth Sciences, 37(3-4), 331-350. https://doi.org/10.1016/J.JAFREARSCI.2003.07.001

Batchelor, R. A., & Bowden, P. (1985). Petrogenetic interpretation of granitoid rock series using multicationic parameters. Chemical Geology, 48(1-4), 43-55. https://doi.org/10.1016/0009-2541(85)90034-8

Bertrand, J. M. L. (1974). Evolution polycyclique des gneiss précambriens de l'Aleksod (Hoggar central, Sahara Algérien). Aspects structuraux, pétrologiques, géochimiques et géochronologiques. USTL Montpellier.

Boissonnas, J. (1973). Les Granites a structures concentriques et quelques autres granites tardifs de la chaine pan-africaine en Ahaggar : Sahara central, Algerie (Centre de recherches sur les zones arides, Éd.). Centre national de la recherche scientifique (France).

Bouabsa, L., Marignac, C., Cuney, M., & Gherbi, C. (2005). The Langhian Granitic Complex of Filfila (North-East Constantine, Algeria) granites in cordierite, granites in tourmaline and granites in metals rare. Mineralogical and Geochemical New Information and petrographical consequences. Bulletin du Service Géologique de l'Algérie, 16(1), 15-53.

Chalal, Y., & Marignac, C. (1997). Discovery of wolframoixiolite in the microgranites in Albite-topaze of Alemeda (Central Hoggar, Algeria) : Metallogenic Implications. Bulletin du Service Géologique de l'Algérie, 8(1), 71-79.

Cheilletz, A., Bertrand, J. M., Charoy, B., Moulahoum, O., Bouabsa, L., Farrar, E., Zimmermann, J. L., Dautel, D., Archibald, D. A., & Boullier, A. M. (1992). Geochimie et geochronologie Rb-Sr, K-Ar et 40 Ar/ 39 Ar des complexes granitiques pan-africains de la region de Tamanrasset (Algerie); relations avec les mineralisations Sn-W associees et l'evolution tectonique du Hoggar central. Bulletin de la Société Géologique de France, 163(6), 733-750.

Cottin, J. Y., Lorand, J. P., Agrinier, P., Bodinier, J. L., & Liégeois, J. P. (1998). Isotopic (O, Sr, Nd) and trace element geochemistry of the Laouni layered intrusions (Pan-African belt, Hoggar, Algeria) : Evidence for post-collisional continental tholeiitic magmas variably contaminated by continental crust. Lithos, 45(1-4), 197-222. https://doi.org/10.1016/S0024-4937(98)00032-2

Cuney, M., Marignac, C., & Weisbrod, A. (1992). The Beauvoir topaz-lepidolite albite granite (Massif Central, France); the disseminated magmatic Sn-Li-Ta-Nb-Be mineralization. Economic Geology, 87(7), 1766-1794. https://doi.org/10.2113/gsecongeo.87.7.1766

De la Roche, H., Leterrier, J., Grandclaude, P., & Marchal, M. (1980). A classification of volcanic and plutonic rocks using R1R2-diagram and major-element analyses—Its relationships with current nomenclature. Chemical Geology, 29(1-4), 183-210. https://doi.org/10.1016/0009-2541(80)90020-0

Debon, F., & Lefort, P. (1988). A Cationic Classification of Common Plutonic Rocks and Their Magmatic Associations : Principles, Method, Applications. Bulletin de Mineralogie, 111, 493-510.

Gravelle, M. (1972). The Great Steps of the History of precambrian in Central Ahhagarand Central-Occidental (Algerian Sahara). Notes et Mémoires du Service Géologique, 236, 41-63.

Gu, L., Zhang, Z., Wu, C., Gou, X., Liao, J., & Yang, H. (2011). A topaz- and amazonite-bearing leucogranite pluton in eastern Xinjiang, NW China and its zoning. Journal of Asian Earth Sciences, 42(5), 885-902. https://doi.org/10.1016/j.jseaes.2010.12.010

Hamis, A., Kesraoui, M., Boutaleb, A., Fuchs, Y., & Marignac, C. (2021). Correction to : Beryl occurrences in the granitic complex of Guerioune, Laouni, Southeastern Algeria: electron microprobe, infrared spectroscopy, and fluid inclusions data. Arabian Journal of Geosciences, 14(7), 578. https://doi.org/10.1007/s12517-021-06960-4

Huang, X. L., Wang, R. C., Chen, X. M., Hu, H., & Liu, C. S. (2002). Vertical variations in the mineralogy of the Yichun topaz lepidolite granite, Jiangxi province, Southern China. The Canadian Mineralogist, 40(4), 1047-1068. https://doi.org/10.2113/gscanmin.40.4.1047

Kamar, M. S. (2015). Geochemistry and mineralizations of the Wadi Ghadir younger granites and associated pegmatites, South Eastern Desert, Egypt. Arabian Journal of Geosciences, 8(3), 1315-1338. https://doi.org/10.1007/s12517-014-1307-0

Kesraoui, M. (2005). Compared Nature and Evolution of Metal Granites Rare in Central Hoggar (Algeria) Through out Petrography, the Cris-

tallochimy of micas and Minerals in Ta, Nb, Sn, W. and geochimy. University of Science and Technology Houari Boumediene, Algiers.

Kesraoui, M., & Nedjari, S. (2002). Contrasting evolution of low-P rare metal granites from two different terranes in the Hoggar area, Algeria. Journal of African Earth Sciences, 34(3-4), 247-257. https://doi.org/10.1016/S0899-5362(02)00023-4

Kovalenko, N. I. (1977). The reactions between granite and aqueous hydrofluoric acid in relation to the origin of fluorine-bearing granites. Geokhimiya, 14, 108-118.

Liégeois, J.-P. (2019). A New Synthetic Geological Map of the Tuareg Shield : An Overview of Its Global Structure and Geological Evolution. In A. Bendaoud, Z. Hamimi, M. Hamoudi, S. Djemai, & B. Zoheir (Éds.), The Geology of the Arab World—An Overview (p. 83-107). Springer International Publishing. https://doi.org/10.1007/978-3-319-96794-3_2

Lin Yin, L., Pollard, P. J., Hu Shouxi, H., & Taylor, R. G. (1995). Geologic and geochemical characteristics of the Yichun Ta-Nb-Li deposit, Jiangxi Province, South China. Economic Geology, 90(3), 577-585. https://doi.org/10.2113/gsecongeo.90.3.577

Luth, W. C., Jahns, R. H., & Tuttle, O. F. (1964). The granite system at pressures of 4 to 10 kilobars. Journal of Geophysical Research (1896-1977), 69(4), 759-773. https://doi.org/10.1029/JZ069i004p00759

Maniar, P. D., & Poccoli, P. M. (1989). Tectonic discrimination of granitoids. Geological Society of America Bulletin, 101(5), 635-643. https://doi.org/10.1130/0016-7606(1989)101<0635:TDOG>2.3.CO;2

Manning, R. B., & Holthuis, L. B. (1981). West African Brachyuran crabs. http://repository.si.edu/xmlui/handle/10088/5652

Masoud, M. S., & Shahin, H. A. A. (2015). Rare-metal enriched peraluminous granite : Examples from south Eastern Desert, Egypt. Arabian Journal of Geosciences, 8(3), 1299-1314. https://doi.org/10.1007/s12517-014-1296-z

McLennan, S. M. (2001). Relationships between the trace element composition of sedimentary rocks and upper continental crust. Geochemistry, Geophysics, Geosystems, 2(4), 1021-1044. https://doi.org/10.1029/2000GC000109

Mohamed, M. A.-M. (2012). Geochemistry and fluid evolution of the peralkaline rare-metal granite, Gabal Gharib, Eastern Desert of Egypt. Arabian Journal of Geosciences, 5(4), 697-712. https://doi.org/10.1007/s12517-010-0244-9

Moulahoum, O. (1988). Duality of Magmatism of Pan-African Age ; Structural Aspects and Petrographics of Sub-Alcalin Granites of Tamanrasset (Cental Hoggar, Algeria). University of Nancy I, France.

Nedjari, S., Kesraoui, M., Marignac, C., & Aissa, D. E. (2001). The Massif of Ebelekan : A granite in Tantale within the South East of Central Hoggar (Algeria). Bulletin du Service Géologique de l'Algérie, 12(1), 15-47.

Pearce, J. A. (1996). Sources and Settings of Granitic Rocks. Episodes, 19(4), 120-125.

Pearce, J. A., Harris, N. B. W., & Tindle, A. G. (1984). Trace Element Discrimination Diagrams for the Tectonic Interpretation of Granitic Rocks. Journal of Petrology, 25(4), 956-983. https://doi.org/10.1093/petrology/25.4.956

Peucat, J. J., Drareni, A., Latouche, L., Deloule, E., & Vidal, P. (2003). U–Pb zircon (TIMS and SIMS) and Sm–Nd whole-rock geochronology of the Gour Oumelalen granulitic basement, Hoggar massif, Tuareg shield, Algeria. Journal of African Earth Sciences, 37(3-4), 229-239. https://doi.org/10.1016/J.JAFREARSCI.2003.03.001

Raimbault, L., Cuney, M., Azencott, C., Duthou, J.-L., & Joron, J. L. (1995). Geochemical evidence for a multistage magmatic genesis of Ta-Sn-Li mineralization in the granite at Beauvoir, French Massif Central. Economic Geology, 90(3), 548-576. https://doi.org/10.2113/gsecongeo.90.3.548

Shand, S. J. (1927). Eruptive Rocks, Their Genesis, Composition Classification and Their Reaction to Ore-Deposits with a chapter on meteorites. Thomas Murby and Co.

SONAREM. (1974). Métaux rares liés aux « apogranites » du Hoggar. [Interne]. SOciété NAtionale de Recherches et d'Exploitation Miniéres.

Stone, M., Exley, C. S., & George, M. C. (1988). Compositions of trioctahedral micas in the Cornubian batholith. Mineralogical Magazine, 52(365), 175-192. https://doi.org/10.1180/minmag.1988.052.365.04

Sylvester, P. J. (1989). Post-Collisional Alkaline Granites. The Journal of Geology, 97(3), 261-280. https://doi.org/10.1086/629302

Taylor, R. P. (1992). Petrological and geochemical characteristics of the Pleasant Ridge zinnwaldite-topaz granite, southern New Brunswick, and comparisons with other topaz-bearing felsic rocks. The Canadian Mineralogist, 30(3), 895-921.

Tischendorf, G., Gottesmann, B., Förster, H.-J., & Trumbull, R. (1997). On Li-bearing micas : Estimating Li from electron microprobe analyses and an improved diagram for graphical representation. Mineralogical Magazine, 61, 809-834.

Tuttle, O. F., & Bowen, N. L. (1958). Origin of Granite in the Light of Experimental Studies in the System $NaAlSi_3O_8$–$KAlSi_3O_8$–SiO_2–H_2O. In O. F. Tuttle & N. L. Bowen (Éds.), Origin of Granite in the Light of Experimental Studies in the System $NaAlSi_3O_8$–$KAlSi_3O_8$–SiO_2–H_2O (Vol. 74, p. 0). Geological Society of America. https://doi.org/10.1130/MEM74-p1

Recived: May 3, 2024
Accepted: June 20, 2024